scientific reports

Check for updates

OPEN

Augmented reality guidance improves accuracy of orthopedic drilling procedures

Frederick Van Gestel[1,2]✉, Fiene Van Aerschot[3,4], Taylor Frantz[5,6], Anouk Verhellen[6,7], Kurt Barbé[8], Bart Jansen[5,6], Jef Vandemeulebroucke[5,6,9], Johnny Duerinck[1,2] & Thierry Scheerlinck[3,4]

In several orthopedic procedures, the accurate use of surgical power tools is critical to avoid damage to surrounding tissues. As such, various guidance techniques and safety measures were developed. Augmented reality (AR) guidance shows promise but requires validation. We evaluated a new approach using an inside-out infrared tracking solution for the HoloLens to compensate for its limited tracking performance. Eighteen participants with varying levels of experience (student, trainee, expert) each drilled twelve trajectories (six perpendicular, six oblique) in equidimensional wooden logs. Three different techniques were evaluated: freehand drilling; proprioception-guided drilling towards the contralateral index finger; and AR-guided drilling using a tracked drill and a virtual overlay of the log with predefined guidance vectors. The angular errors between planned and performed trajectories were compared using a mixed-design ANOVA. The results demonstrated that guidance technique ($p < 0.001$) and drilling direction ($p < 0.001$) significantly affected drilling accuracy, while experience ($p = 0.75$) did not. AR outperformed both other techniques, particularly for oblique trajectories ($p < 0.001$). For perpendicular trajectories, it only outperformed proprioception guidance ($p = 0.04$). Target plots revealed an important scatter perpendicular to the longitudinal axis of the log during freehand and proprioception-guided drilling, especially for oblique trajectories. This inaccuracy disappeared during AR-guided drilling. As such, we were able to conclude that AR guidance using inside-out infrared tracking reduced angular uncertainty during directional drilling, resulting in improved drilling accuracy. This improvement was particularly noticeable for complex trajectories and angles. The benefits of AR guidance were observed across all experience levels, highlighting its potential for orthopedic applications. We believe this study opens the way for the methodical evaluation of AR guidance in specific orthopedic use cases.

Keywords Augmented reality, Orthopedic drilling, Navigation, HoloLens, Computer-assisted surgery

Accuracy in drilling plays an important role across various domains of orthopedics and traumatology, with applications such as sacroiliac screw placement in pelvic fracture cases, guiding pin insertion for optimal implant positioning in total shoulder or femoral head resurfacing arthroplasties, and pedicle screw placement in spine surgeries. During such procedures, improper use of surgical power tools can cause inaccuracies and harm nearby soft tissues[1–6]. To address this, various aiming techniques and safety measures were developed. During freehand drilling without additional guidance the grip on the drill can help estimate the trajectory[7]. *Clenched grip* involves clenching the handle with the entire hand, while *shooting grip* uses the index finger of

[1]Department of Neurosurgery, Universitair Ziekenhuis Brussel (UZ Brussel), Vrije Universiteit Brussel (VUB), Laarbeeklaan 101, 1090 Brussels, Belgium. [2]Research Group Center For Neurosciences (C4N-NEUR), Vrije Universiteit Brussel (VUB), Laarbeeklaan 103, 1090 Brussels, Belgium. [3]Department of Orthopedic Surgery and Traumatology, Universitair Ziekenhuis Brussel (UZ Brussel), Vrije Universiteit Brussel (VUB), Laarbeeklaan 101, 1090 Brussels, Belgium. [4]Research Group Beeldvorming en Fysische Wetenschappen (BEFY-ORTHO), Vrije Universiteit Brussel (VUB), Laarbeeklaan 103, 1090 Brussels, Belgium. [5]Department of Electronics and Informatics (ETRO), Vrije Universiteit Brussel (VUB), Pleinlaan 9, 1050 Brussels, Belgium. [6]imec, Kapeldreef 75, 3001 Leuven, Belgium. [7]Department of Studies on Media, Innovation and Technology (SMIT), Vrije Universiteit Brussel (VUB), Pleinlaan 9, 1050 Brussels, Belgium. [8]Department of Public Health, Research Group Biostatistics and Medical Informatics (BISI), Vrije Universiteit Brussel (VUB), Laarbeeklaan 103, 1090 Brussels, Belgium. [9]Department of Radiology, Vrije Universiteit Brussel (VUB), Universitair Ziekenhuis Brussel (UZ Brussel), Laarbeeklaan 101, 1090 Brussels, Belgium. ✉email: frederick.vangestel@uzbrussel.be

that hand as aiming support pointing in the drill bit's direction. Palpation of the target with the opposite index finger provides additional guidance through proprioceptive feedback, enhancing performance in comparison to freehand drilling[7]. However, palpating the target is not always feasible.

While 3D-printed guides ensure a predefined trajectory, they are expensive, time-consuming, and require a well-organized workflow[8–11]. Additionally, outsourcing planning and printing makes them unavailable for emergencies. Alternatively, conventional intraoperative navigation devices, using infrared tracking through a stereoscopic camera to provide a link between the physical world and imaging information (both pre- and intraoperatively obtained), have shown to improve surgical accuracy by allowing the surgeon or a robotic assistant to follow certain predefined trajectories and take the surrounding tissues into account[12–14]. Nevertheless, these systems are often bulky (with a sizeable screen, camera and/or computer unit), expensive, and time-consuming, limiting their use in orthopedic surgery[13,14].

Augmented reality (AR) is a technology which allows superposition of information atop the real world and has been an evolving field of research since the mid-1990s. During the last decade, several portable and fully integrated AR devices have become available, providing the wearer with virtual 3D data integration into their environment. Such devices allow the surgeon to view pre- and/or intraoperative image information and measurements in full 3D, superposed on or next to the patient; the virtual image commonly called 'hologram'. Initial attempts at implementing this technology in surgical routines often involved manual hologram registration, stabilized in space using the simultaneous localization and mapping algorithms of the head-mounted device (HMD)[15–17]. However, their tracking performance is a well-known limitation of such off-the-shelf hardware; often several centimeters, falling short of the millimeter scale tracking required for surgical navigation, leaving the advantage of AR guidance uncertain.

To overcome these challenges in drilling based surgical tasks, we developed a navigation approach using the HoloLens (Microsoft Corporation, USA)[18–22]. With the goal of precise operative tracking in mind, several studies have adopted tracking of QR-code markers using the device's integrated RGB sensor[18,23–28]. However, these markers are often large and difficult to integrate into a surgical workflow due to sterility requirements. Moreover, the RGB sensor within the HoloLens has a limited field of view which makes consistent tracking of these markers difficult[19]. Infrared-based tracking approaches, on the other hand, can be integrated easily thanks to the widespread use of infrared tracking by conventional navigation systems, while the HoloLens' infrared sensor also provides a larger field of view. Additionally, by adopting an inside-out approach to tracking, the system remains fully portable and does not depend on ancillary tracking hardware such as an external camera. As such, these approaches have previously demonstrated millimetric performance in tracking existing surgical hardware[20–22,29–31]. To address the off-the-shelf tracking limitations of the AR-HMD, we integrated prior work on inside-out tracking of infrared-reflective markers using the HoloLens' on-board infrared sensor[19–22]. This allowed accurate tracking (mean tracking error of 0.78 mm ± 0.74 mm; *unpublished Vicon validation testing*) of instrumentation, and image registration (mean registration error of 1.42 mm ± 0.42 mm and 0.95° ± 0.36°; a cumulative error integrating – among others – the tracking error and the surgeon error)[22]. As such, a stable coordinate frame was provided for both registration and data interpretation of additional imaging and planning information, such as drilling trajectories. We evaluated our approach by comparing the angular accuracy of three drilling techniques: freehand drilling, proprioception-assisted drilling, and AR-assisted drilling.

Methods

Ethical review and compliance

The research protocol was reviewed by the *Commissie Medische Ethiek Universitair Ziekenhuis Brussel*, the ethics committee of the University Hospital Brussels. Since the study did not involve any human or animal test subjects, only human participants performing the testing and not undergoing any individual analyses, the need for ethical approval was waived. All research was performed in accordance with relevant guidelines and regulations, as well as the Declaration of Helsinki. All researchers were in possession of a certificate of Good Clinical Practice.

Participants

Eighteen participants were recruited: six medical master students, six orthopedic trainees and six experienced orthopedic surgeons. None had extensive AR or navigation experience, but some had previous exposure. Each received brief, standardized training on the HoloLens and software workflow. All signed informed consent and completed pre- and post-experiment questionnaires assessing previous AR and bone drilling experience.

Drilling protocol

To minimize the influence of irregular bone specimens or models on drilling performance, we opted for a low-cost and low-variable wooden log model. Each participant drilled 12 trajectories in equidimensional wooden logs measuring 60 × 500 mm. Participants used a battery-driven GRS 12 V-15 drill (Robert Bosch GmbH, Germany) with a 2.5 × 95 mm bit, resembling a drill used in orthopedic procedures. Each trajectory was defined by an "entry" and "exit" point in the same cross-sectional YZ-plane, with the Z-axis indicating the perpendicular drilling direction (Fig. 1). All 12 exit points were aligned along the log's longitudinal X-axis. Six of the entry points were located on a line opposite the exit points (perpendicular to the XY-plane). The six remaining points were located about 1 cm on each side of that line (oblique to the XY-plane). Entry and exit points were marked by a 2.5 mm predrilled cavity of 2 mm—3 mm depth to make them visible on CT scans. The wooden logs were securely fastened to a workbench, with all the exit holes at the lowest point of the log. To simulate limited exposure in the operating field, a fenestrated cloth covered the logs, revealing only the entry points.

Before commencing the experiment, participants had the opportunity to examine the precise placement of the entry and exit holes both on diagrams of the log (Fig. 1) and on the physical log itself. This ensured that all participants understood that the target holes were positioned at the lowest point of the log, with the entry holes

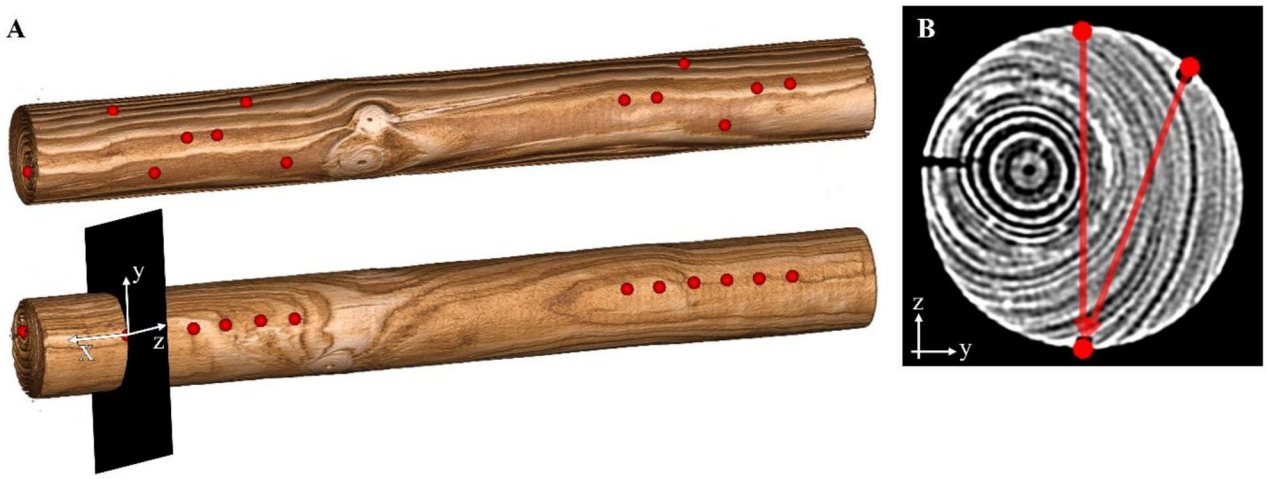

Fig. 1. (**A**) 3D models of one of the wooden logs with the planned entry (top) and exit (bottom) points defining 12 different trajectories. Each set of entry and exit points (both for perpendicular and oblique trajectories) is located in the same cross-sectional YZ-plane. (**B**) CT scan of the log with a cross-sectional view (YZ-plane) showing an example of both a perpendicular and an oblique trajectory (entry points located at the top of the image).

located either at the highest point (perpendicular trajectories) or 1 cm to either side (oblique trajectories). Each participant drilled two perpendicular and two oblique trajectories with each of the three guidance techniques: freehand drilling, proprioception-guided and AR-guided drilling. During freehand drilling, participants did not receive supplementary guidance other than the information they received beforehand. In the second setting, participants drilled based on tactile and proprioceptive feedback on the exit point using the contralateral index finger. For the AR guided technique, participants used the HoloLens to project an AR overlay of the predefined guidance vectors registered to the log (Fig. 2). The sequence of guidance techniques was randomly assigned to prevent any potential learning bias.

Augmented reality

We developed a software workflow for AR-guided drilling on the HoloLens using the Unity development platform (Unity Technologies, USA). The process involved acquiring a CT scan of the wooden logs using a standard preoperative diagnostics protocol: CT scanner, SOMATOM Definition AS (Siemens, Munich, Germany); collimation, 6×0.75 mm; adjacent slices; slice thickness, 0.6 mm; reconstructed slice interval, 0.6 mm; tube potential, 70 kVp; tube current, 160 mA; convolution kernel, B80S ultra sharp; and field of view, 120 mm. From this scan, we generated a 3D surface model of the log and created virtual guidance vectors between the entry and exit points using the open-source 3D Slicer software package (version 4.10, http://www.slicer.org). To track the physical objects, including the log, the drill, and a stylus, we equipped them with a unique constellation of five disposable infrared-reflective marker spheres (Northern Digital Incorporated, Canada), which was tracked by the infrared camera of the HoloLens.

To determine the participant's interpupillary distance, we employed the standard HoloLens' eye calibration procedure. Subsequently, calibration between the HMD display and wearer eyes was performed, adopting the workflow of Azimi et al.[32]. This was done by aligning an IR tracked reference frame with its silhouette visible on the AR display. Fine-tuning this visualization calibration to accommodate for variations in interpupillary distance and HoloLens positioning was performed by manually adjusting the virtual silhouette until it accurately matched the spatial position of its real-world counterpart. Additionally, we developed a custom-made calibration object equipped with infrared-reflective markers to precisely identify the drill bit's orientation and location of its tip.

To register the virtual 3D model of the log and guidance vectors to the physical world, participants pointed the tip of the infrared-tracked stylus at each of the 12 entry points, as well as an additional point at each end of the log. We then employed a pose estimation technique using the point-pairs least squares optimization method to align the virtual and real-world objects. The quality of the registration was monitored by calculating the mean registration error between the 3D model and the 14 sampled points. Within the AR display, points within 2 mm of their registered target were rendered in green, those between 2 and 4 mm in orange, and those over 4 mm in red. This allowed easy identification of outlier data, as points could be replaced. The registration process was refined until a mean fiducial registration error below 3.5 mm was achieved, and the AR log visually overlaid the real log.

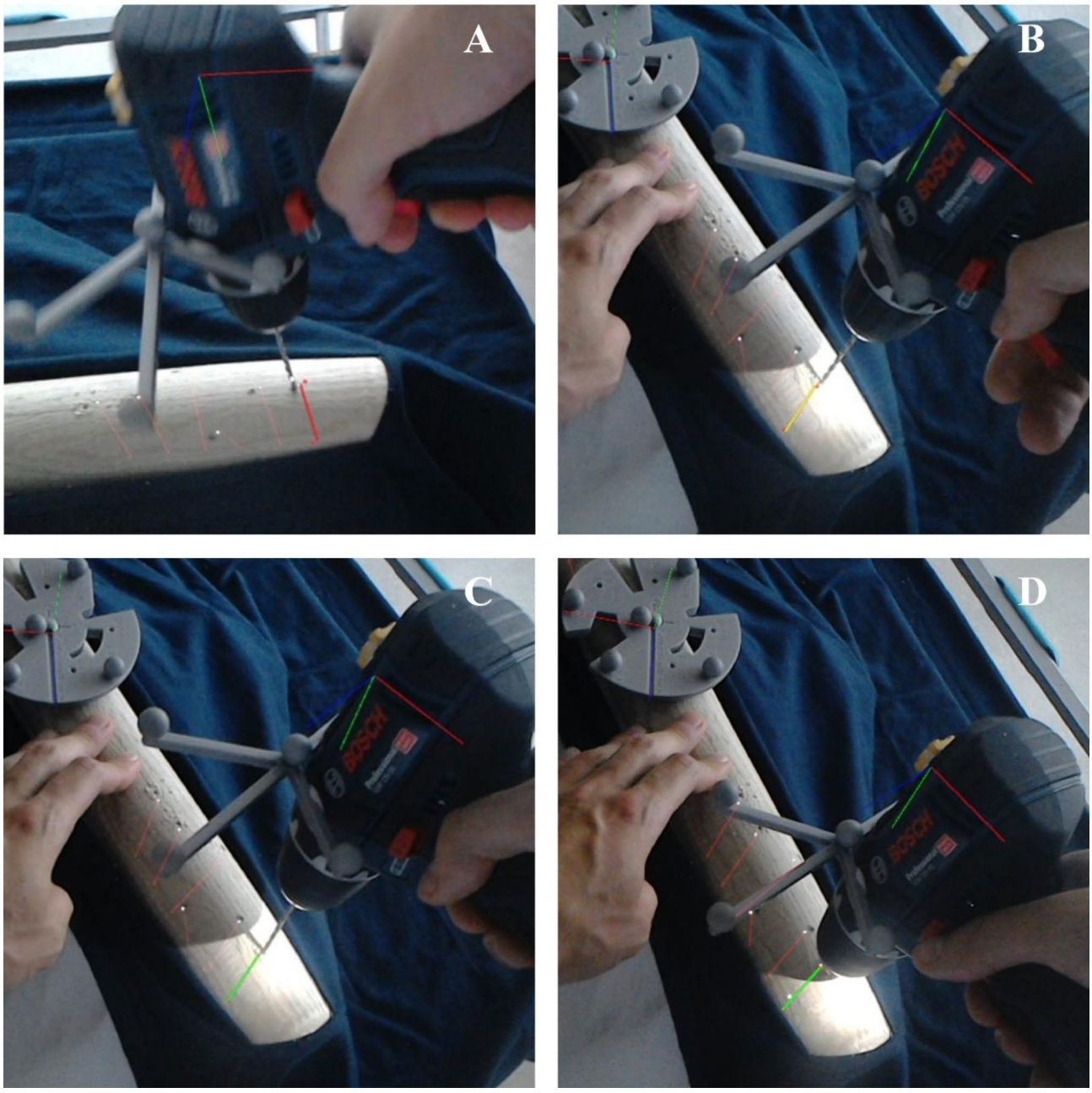

Fig. 2. Drilling procedure using AR guidance. The log and drill are tracked by infrared-reflective marker spheres, providing the spatial position and orientation of the log's planned guidance vectors (in faded red) and the drill. (**A**) When the drill was approximated to the selected guidance vector, but aligned outside the 4° threshold, the vector would light up red. (**B**) When alignment was between 2° and 4° it would turn orange and (**C**) under 2° it would turn green. (**D**) During drilling the vector's color continued to indicate the drill alignment, while drill tip advancement inside the log could be monitored through a virtual white sphere displayed at the drill tip, that progressed along the virtual trajectory as the drill advanced.

AR-guided drilling

During the AR drilling process, participants positioned the drill at the entry point and aligned the drill bit with the corresponding guidance vector. As soon as the trajectory of the drill matched the guidance vector within a tolerance of 4°, the color of the vector changed from red to orange. When the alignment was within 2°, the vector changed to green, indicating that the drilling direction was appropriate. Visual feedback helped in finding the correct direction. Throughout the drilling process, the color of the vector continued to indicate the alignment, while a virtual white sphere displayed at the drill tip allowed participants to monitor the drill's advancement inside the log along the virtual trajectory (Fig. 2).

Outcome

During the experiment, we assessed drilling performance in terms of error magnitude and error direction. To acquire these values, we respectively measured the radial distance (r) and polar angle (θ) of each exit point (O) in relation to the target point (T). Two blinded investigators (FVG, FVA) measured the values independently. If the measurements differed within 1 mm for r and 5° for θ, we averaged the results. Otherwise, both investigators remeasured together and reached a consensus. An error magnitude below 0.1 mm without a discernable error direction was considered an on-target drilling performance. The error between planned and performed entry points was not measured as they were predrilled and the error therefore insignificant.

Error magnitude

We used digital calipers (accuracy: 0.02 mm) to measure the shortest radial distance (r) between the centers of the targeted (T) and obtained (O) drill holes (Fig. 3A). The deviation angle (α) between the planned (ET) and obtained (EO) trajectories, calculated based on the inscribed angle theorem to account for the log's radius (*rad*), represented the error magnitude[33].

Error direction

A 2D polar coordinate system was established, with T as the pole and the log's longitudinal X-axis as the polar x-axis (Fig. 3B). Using a goniometer, we measured the polar angle (θ) between the polar axis and the line (r) connecting the targeted (T) and obtained (O) exit points. By applying trigonometric functions, we converted the radial distance (r) and polar angle (θ) of each exit point (O) to their cartesian coordinates (x, y) relative to the planned target point (T). This conversion was necessary for analyzing the error direction.

Statistical analysis

Statistical analysis was divided into two parts: the first part analyzed deviation angle α, representing error magnitude, in terms of accuracy and precision, while the second part analyzed the spread of cartesian coordinates x, y, representing error direction. Categorical data were compared using a χ^2 test. Statistical analyses were performed using SPSS Statistics software version 26 (International Business Machines Corporation, USA) and Prism 9.0.0 (GraphPad Software, USA) for graph creation. Significance was defined as $p < 0.05$.

Error magnitude

To assess performance accuracy, we compared deviation angle sizes as ratio variables using means, standard deviations (SD), minimums (Min), and maximums (Max). Given the collection of both between-subject (experience level) and within-subject factors (guidance technique, drilling direction, repeated measures), a mixed-design analysis of variance (ANOVA) with random intercepts was applied, considering α as dependent variable and guidance technique, experience level, and drilling direction as predictors. Interactions between predictors were also analyzed. Pairwise tests with Bonferroni correction (more conservative, requiring stronger evidential value) were conducted to explore the origin of significant differences.

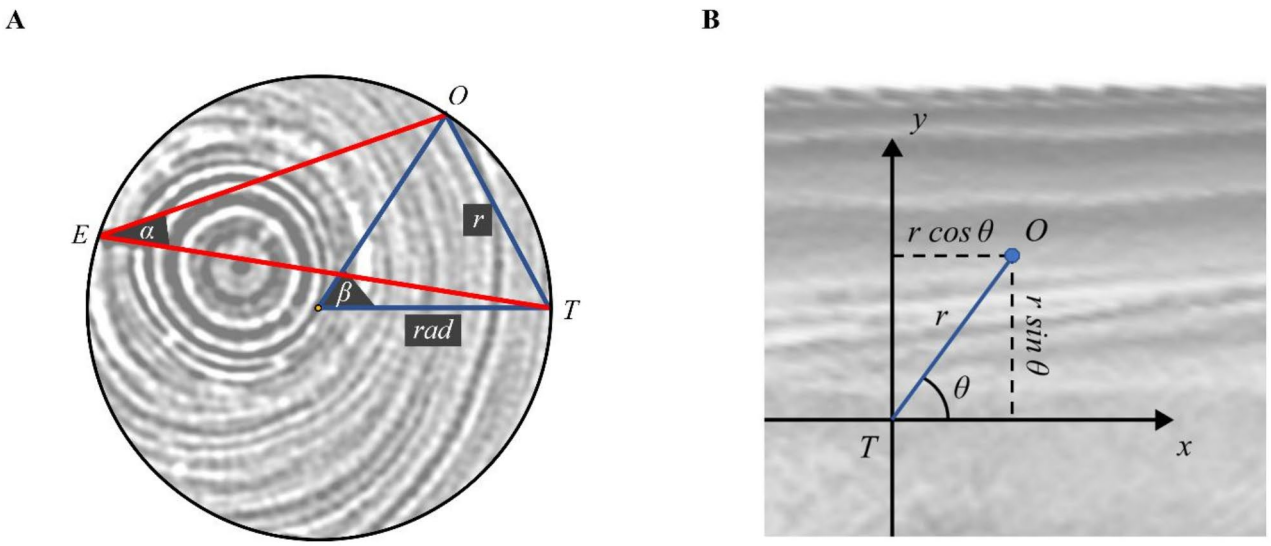

Fig. 3. Outcome parameters of directional drilling. (**A**) Cross-sectional view of the log with planned (ET) and obtained (EO) trajectories. Using the inscribed angle theorem, the deviation angle (α) was calculated based on the log's radius (rad) and the radial distance (r) between the target (T) and the outcome (O). (**B**) Side view of the log with the longitudinal X-axis of the log as the polar x-axis. The targeted exit point (T) was set as the pole and the x-axis as the polar axis. Using trigonometric functions, the polar coordinates (r, θ) of the obtained exit point (O) were calculated.

To assess performance precision, we evaluated the proximity between obtained exit points with the same predictors. Only two attempts were available for each predictor combination, meaning variance of the individual deviation angles could not be assessed. Instead, we used the calculated distance between the two attempts as a measure of precision and repeatability for that predictor combination. Abovementioned ANOVA and pairwise testing were used to compare these distances.

Error direction

We examined the relative scatter of exit points along the x- and y-axes through their corresponding cartesian coordinates (*x, y*) in terms of variance and covariance. The coordinates were transformed into a single complex variable with normal distribution using imaginary numbers ($p = x + i \cdot y$), which was analyzed using a compound symmetry covariance structure (aiming for the smallest Akaike's Information Criterion (AIC))[34]. Compound symmetry implies that all variances and covariances would be equal, resulting in an equal distribution of the coordinates along both axes. We assessed the relation to predictors and their interactions to determine the criteria minimizing AIC. Heterogeneous compound symmetry in the resulting covariance matrices indicated preferential scattering along one axis. Likelihood-ratio tests were performed to investigate the origin of significant differences.

Results

Participants

We recruited eighteen participants: six medical master students, six orthopedic trainees and six orthopedic surgeons (Table 1). All medical students had an interest in orthopedic surgery, though one was replaced because of a red-green color vision deficiency interfering with the AR guidance. The level of reported experience with bone drilling ($p = 0.011$) as well as the age ($p < 0.001$) were correlated to the participants' experience level, which was to be expected. This was not the case for the participants' sex, nor their experience with the HoloLens. None of the participants had extensive experience with AR before the experiment, but 5/18 had used some form of AR before (Table 1).

Impact of technique, experience and drilling direction on error magnitude

Performance accuracy

The mean overall accuracy, i.e. the mean angular deviation between planned and achieved trajectories of all measurements (quantifying the extent of deviation from the target regardless of the size of the drilled medium), was 5.14° (SD: 4.04°, Min. 0.00°—Max. 21.44°). Accuracy was significantly impacted by the guidance technique (mixed-model ANOVA, $p < 0.001$) and the drilling direction ($p < 0.001$), but not by the level of experience ($p = 0.75$) (Table 2). Only the interaction between guidance technique and drilling direction was significant ($p = 0.037$). Although there was no significant effect from the participants' experience level, we noticed that experts had the best overall performance when using AR guidance, both for perpendicular trajectories at 2.81° (SD: 1.32°, Min. 0.00°—Max. 4.90°) and oblique trajectories at 2.96° (SD: 1.57°, Min. 0.82°—Max. 5.55°).

The pairwise tests, with Bonferroni correction for multiple comparisons, indicated that AR performed significantly better than both proprioception-guided and freehanded drilling (both pairwise comparisons: $p < 0.001$). However, there was no significant difference between proprioception-guided and freehanded drilling ($p = 0.14$). As the interaction between the guidance technique and the drilling direction was significant, we compared the marginal means of the deviation angles for the subgroups to identify the source of significance (Table 3, Fig. 4). Looking within each drilling direction subgroup, the results showed that for perpendicular drilling directions the accuracy obtained through AR guidance was significantly better than proprioception-guided drilling ($p = 0.04$), while for oblique drilling directions it outperformed both techniques (both $p < 0.001$). Looking within each guidance technique subgroup, the difference between the accuracy for perpendicular versus oblique drilling directions was only significant in the proprioception-guided subgroup, in favor of perpendicular drilling directions ($p < 0.001$). All other comparisons were not significant.

Out of a total of 216 drillings, 5 (2.31%) were on-target ($r < 0.1$ mm). None of the drillings were on-target in the freehand group, 1 in the proprioception group and 4 in the AR group (χ^2, $p = 0.074$).

		Student	Trainee	Surgeon	P-value
Mean age in years (SD, Min–Max)		**24.3 (1.03, 23–26)**	**29.5 (2.17, 26–32)**	**43.7 (8.04, 32–53)**	$p < 0.001$
Sex	Male	5	4	2	χ^2 (2, $n = 18$) = 3.27 $p = 0.19$
	Female	1	2	4	
Experience in bone drilling	None	4	0	0	χ^2 (6, $n = 18$) = 16.67 $p = 0.011$
	Some	2	2	0	
	Considerable	0	4	5	
	Very experienced	0	0	1	
Use of HoloLens before	Yes	1	3	1	χ^2 (2, $n = 18$) = 2.22 $p = 0.33$
	No	5	3	5	

Table 1. Participant characteristics.

Predictor		Angular error (α) in °	ANOVA		
			F-value	p-value	
Guidance technique	Freehand	5.75 ± 3.68 (0.34–19.21)	20.27	< 0.001	Interaction: p = 0.037
	Proprioception	6.86 ± 4.66 (0.00–21.44)			
	Augmented Reality	3.38 ± 2.19 (0.00–7.85)			
Experience level	Student	5.34 ± 3.67 (0.00–15.24)	0.289	0.75	
	Trainee	4.98 ± 3.68 (0.00–20.80)			
	Expert	5.67 ± 4.38 (0.00–21.44)			
Drilling direction	Perpendicular	4.52 ± 2.55 (0.00–11.61)	12.65	< 0.001	Interaction: p = 0.037
	Oblique	6.14 ± 4.80 (0.00–21.44)			

Table 2. Orthopedic drilling performance. Accuracy of orthopedic drilling grouped by guidance technique, experience level and drilling direction (mean ± SD (Min–Max)), with the ANOVA results on the right.

		Guidance technique		
		Freehand	Proprioception	Augmented Reality
Drilling direction	Perpendicular	4.95 ± 2.58 (4.07–5.82)	5.32 ± 2.69 (4.41–6.23)	3.28 ± 1.91 (2.64–3.93)
	Oblique	6.55 ± 4.42 (5.05–8.05)	8.40 ± 5.65 (6.49–10.31)	3.47 ± 2.46 (2.64–4.30)

Table 3. Subgroup deviation angles. Subgroup deviation angles for each combination of guidance technique and drilling direction (mean ± SD (95% confidence interval between brackets) expressed in degrees).

Performance precision

Overall, the mean precision of our experiment, i.e. the mean distance between the two achieved exit points with a same set of predictors (quantifying the proximity of these points), was 6.71 mm (SD 6.93 mm, Min. 0.11 mm—Max. 36.40 mm). In general, perpendicular drilling was more precise than oblique drilling (mixed-model ANOVA, $p < 0.001$). However, guidance technique ($p = 0.56$) or level of experience ($p = 0.23$) had no significant impact.

Impact of technique, experience and drilling direction on error direction

As experience had no significant impact on accuracy, we grouped experience level data and produced target plots for perpendicular and oblique drilling within each guidance technique subgroup (Fig. 5). These plots showed that during freehand and proprioception-guided drilling, the scatter along the Y-axis was larger than along the X-axis. This was especially true for oblique drilling. On the other hand, AR-guided drilling resulted in a visually smaller and more uniform scatter along both axes. This was confirmed through the heterogenous compound symmetry analyses of their respective (co)variance matrices, with a clear AR-induced scatter reduction (lower mean, smaller 95% CI). Surprisingly, when combining all techniques, the experts performed worse along the X-axis but better along the Y-axis. As the difficulty was introduced mainly along the Y-axis, requiring more focus, this performance dichotomy could indicate a confidence bias for simpler situations in the expert group.

The overall model showed a significant variance ($p = 0.032$), indicating large inter- and intra-participant performance variabilities. AR reduced those variabilities, especially for the outliers. Additionally, the intra-participant changes in variance that occur during sequentially drilling with the different techniques remained similar for all participants, indicating the absence of a learning effect.

Discussion

The use of AR guidance for directional drilling yielded a higher angular accuracy compared to freehand and proprioceptive guidance. Regardless of experience, AR reduced the angular error by nearly half and led to more on-target drilling outcomes. Particularly in oblique drilling, AR proved highly beneficial, greatly reducing scatter along the Y-axis. This can be attributed to the intuitive ease of drilling perpendicularly based on visual information, as opposed to drilling along a less clearly defined path.

In contrast to Langeveld et al.[7], our study found no significant improvement caused by proprioceptive feedback or experience. Surprisingly, the expert orthopedic surgeons performed relatively poorly using both current guidance techniques, while trainees and even master students performed better. This discrepancy may be attributed to a confidence bias exhibited by the expert group in such a common situation. Experts often performed quickly between their day-to-day tasks, while the student and trainee groups had a stronger incentive to perform their best under staff supervision. However, when faced with a new element or added difficulty, such as the introduction of AR guidance, the experts outperformed all other groups. This observation highlights the influence of experience, which was masked by the confidence bias when using the current guidance techniques.

One significant limitation of our study was the utilization of a simple, non-anatomic phantom model. The decision to utilize wooden logs rather than anatomical bone models was deliberate and aimed at isolating the

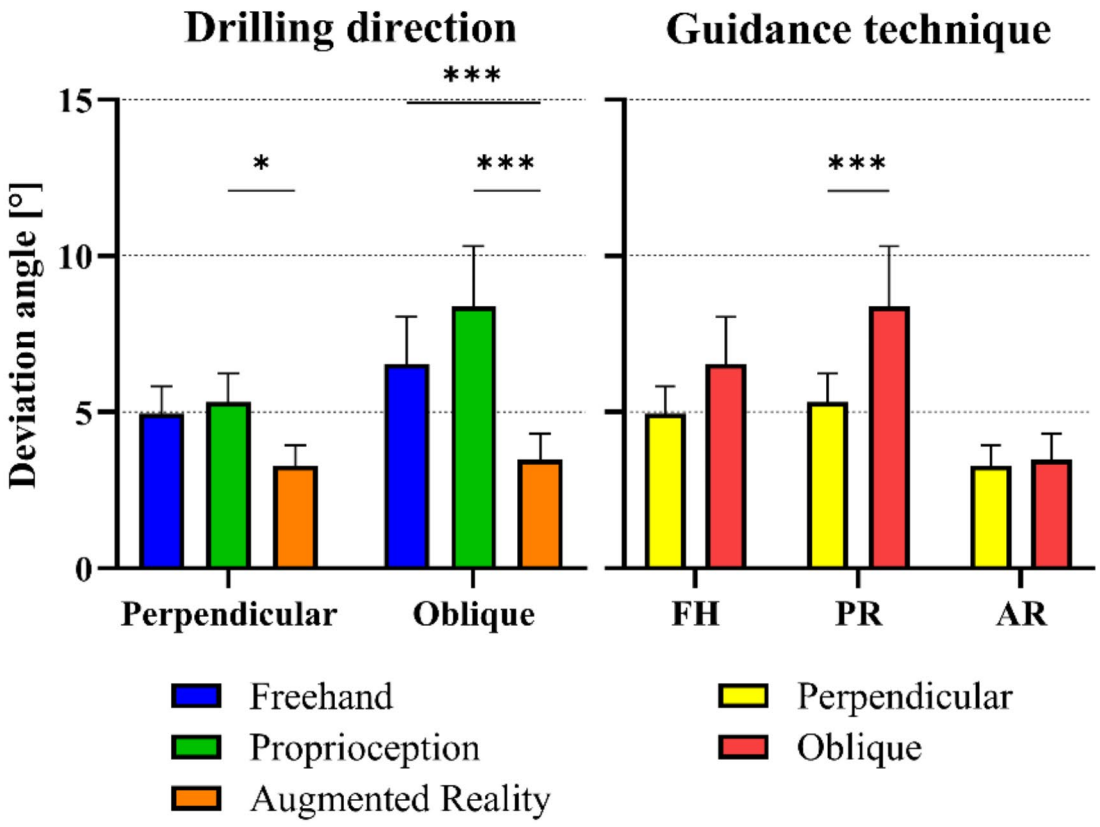

Fig. 4. Subgroup analyses to identify the source of significance within the drilling direction (left) and guidance technique (right) subgroups. The mean deviation angles (value along y-axis, expressed in degrees, error bars representing the 95% confidence interval) within each drilling direction (perpendicular, oblique) and guidance technique (freehand, proprioception, AR) subgroup were compared for significance. Each of these analyses was performed only within their respective subgroup. FH = freehand; PR = proprioception; AR = augmented reality; * = $p < 0.05$; *** = $p < 0.001$.

variable of interest, i.e. drilling performance, without introducing additional influences or confounding factors that could potentially obscure the nuanced assessment of drilling proficiency. To achieve this, we opted for equidimensional wooden logs as our experimental medium, ensuring uniform measurements across the entire phantom by eliminating variables such as thickness variations and diverse shapes that are inherent to anatomical bone models. For the same reason, we did not simulate intraoperative factors that could affect performance, such as surrounding soft tissues and scialytic light. A second limitation was the presence of pre-drilled entry holes in the phantom, which were used for planning. As a consequence, our experiment only evaluated aiming performance and not the ability to locate the entry point, which could prove challenging for both current and AR-guided drilling techniques. Another limitation was our focus solely on the final cumulative error, without considering the tracking error by the AR system and the registration error by the participant. Though internal testing found the tracking error to be sufficiently low (0.78 mm ± 0.74 mm), the registration error could introduce variability as it was performed by each participant individually. Nonetheless, considering that this step is common in navigated surgeries and contributes to the overall system performance, we believe it should be acknowledged as an inherent part of the final error.

Nevertheless, AR presents a promising alternative to the existing navigation systems, which lack the ergonomics and ease-of-use for widespread adoption in orthopedic surgery. By utilizing AR HMDs with inside-out tracking, navigation could become more lightweight and cost-effective, potentially mitigating line-of-sight issues[24]. Furthermore, the compact size of AR HMDs opens up possibilities for exploring applications beyond the operating room. However, certain challenges must be addressed before widespread implementation becomes feasible[35]. Firstly, in the authors' experience, the use of the HoloLens by individuals with glasses is challenging at times, depending on the wearer's corrective lens frame geometry. In such cases, it can be difficult to position the HMD correctly with respect to the wearer's eyes such that an optimal view through the device is guaranteed, making the combined use during surgery somewhat impractical. Additionally, visualization design can have an

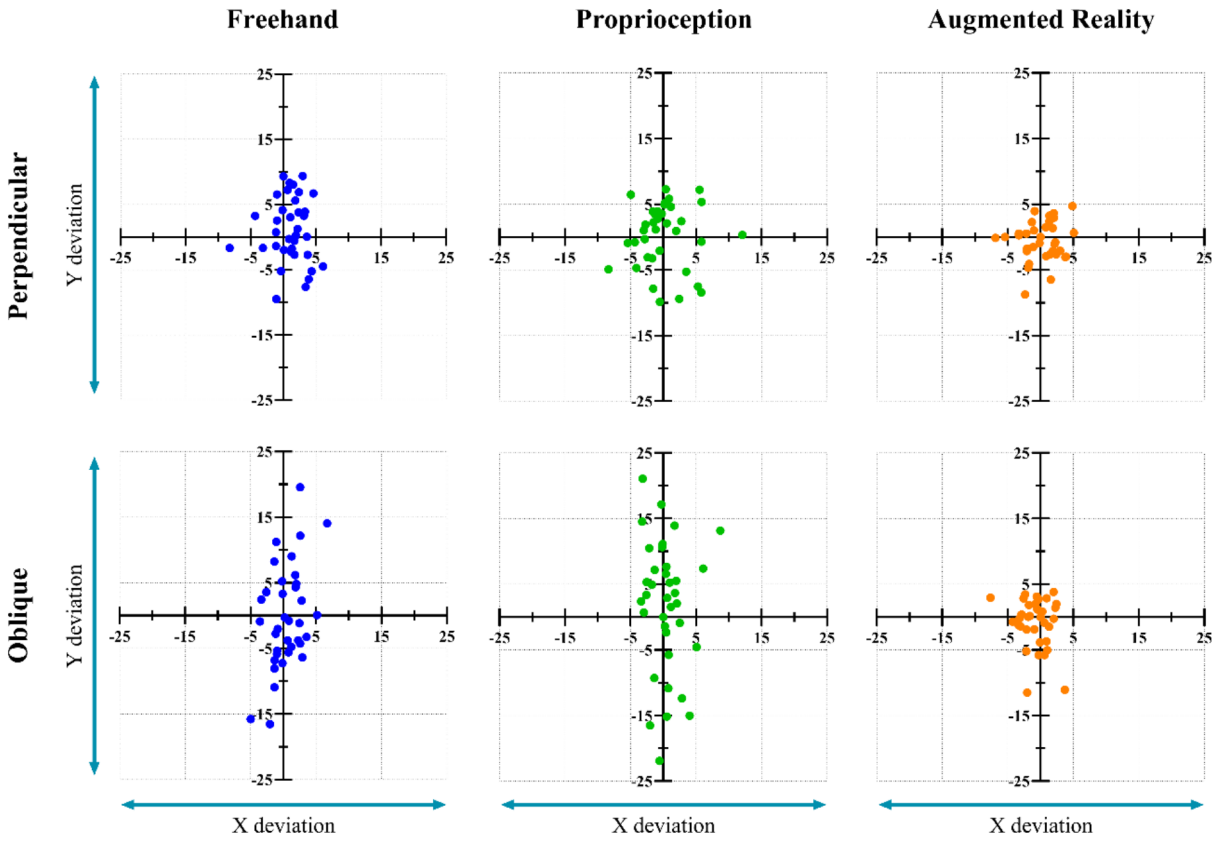

Fig. 5. Target plots showing the achieved end points for each combination of guidance technique and drilling direction. End points are plotted relative to the planned target point, indicated as each zero point. Axes correspond to the XY plane, tangent to the planned target point (as seen in Figs. 1A and 3B), onto which the relative position of the achieved end points is projected, indicating the deviation in each axis direction in millimeters.

important influence on performance, as shown by Wolf et al.[36], and should therefore be tailored to each specific use case. Secondly, AR-based navigation would require medical device certification. Most current AR HMDs, including the HoloLens, are off-the-shelf devices not specifically tailored for medical use. Lastly, before AR can be widely adopted in everyday surgical settings, it needs to undergo validation in a more clinical environment, such as testing on anatomical specimens, performing a direct comparison with gold-standard navigation solutions, optimizing the user interface for the operating room environment, and conducting performance evaluations through patient trials[37].

Conclusion

AR guidance using inside-out infrared tracking reduced angular uncertainty during directional drilling, resulting in improved drilling accuracy. This improvement was particularly noticeable for complex trajectories and angles. The benefits of AR guidance were observed across all experience levels, highlighting its potential for orthopedic applications. We believe this study opens the way for the methodical evaluation of AR guidance in specific orthopedic use cases.

Data availability

Upon request, please contact Dr. Frederick Van Gestel.

Received: 10 September 2023; Accepted: 10 October 2024
Published online: 25 October 2024

References

1. Dietze, S., Perka, C. & Baecker, H. Gefäß- und nervenverletzungen in der hüftendoprothetik. *Orthopäde* **43**(1), 64–69. https://doi.org/10.1007/s00132-013-2126-9 (2014).
2. Abdul-Jabbar, A. et al. Neurovascular relationships of S2AI screw placement: Anatomic study. *World Neurosurg.* **116**, e108–e112. https://doi.org/10.1016/j.wneu.2018.04.095 (2018).

3. Han, C. D. et al. Relationship between distal screws and femoral arteries in closed hip nailing on computed tomography angiography. *Arch. Orthop. Trauma Surg.* **133**(3), 361–366. https://doi.org/10.1007/s00402-012-1674-5 (2013).
4. Iorio, J. A., Jakoi, A. M. & Rehman, S. Percutaneous sacroiliac screw fixation of the posterior pelvic ring. *Orthop. Clin. N. Am.* **46**(4), 511–521. https://doi.org/10.1016/j.ocl.2015.06.005 (2015).
5. Robinson, L., Persico, F., Lorenz, E. & Seligson, D. Clavicular caution: an anatomic study of neurovascular structures. *Injury* **45**(12), 1867–1869. https://doi.org/10.1016/j.injury.2014.08.031 (2014).
6. Gertzbein, S. D. & Robbins, S. E. Accuracy of pedicular screw placement in vivo. *Spine* **15**(1), 11–14. https://doi.org/10.1097/00007632-199001000-00004 (1990).
7. Langeveld, A. R. J., Rustenburg, C. M. E., Hoozemans, M. J. M., Burger, B. J. & Meuffels, D. E. To improve your surgical drilling skills, make use of your index fingers. *Clin. Orthop. Relat. Res.* **477**(1), 232–239. https://doi.org/10.1097/corr.0000000000000557 (2019).
8. Rankin, I., Rehman, H. & Frame, M. 3D-printed patient-specific ACL femoral tunnel guide from MRI. *Open Orthop. J.* **12**, 59–68 (2018).
9. Yang, J. C. et al. Clinical experience using a 3D-printed patient-specific instrument for medial opening wedge high tibial osteotomy. *Biomed. Res. Int.* **2018**, 9246529. https://doi.org/10.1155/2018/9246529 (2018).
10. Marengo, N. et al. Cortical bone trajectory screw placement accuracy with a patient-matched 3-dimensional printed guide in lumbar spinal surgery: A clinical study. *World Neurosurg.* **130**, e98-104. https://doi.org/10.1016/j.wneu.2019.05.241 (2019).
11. Audenaert, E. et al. A custom-made guide for femoral component positioning in hip resurfacing arthroplasty: Development and validation study. *Comput. Aided Surg.* **16**(6), 304–309. https://doi.org/10.3109/10929088.2011.613951 (2011).
12. Mezger, U., Jendrewski, C. & Bartels, M. Navigation in surgery. *Langenbecks Arch. Surg.* **398**(4), 501–514. https://doi.org/10.1007/s00423-013-1059-4 (2013).
13. Kumar, V., Patel, S., Baburaj, V., Rajnish, R. K. & Aggarwal, S. Does robotic-assisted surgery improve outcomes of total hip arthroplasty compared to manual technique? A systematic review and meta-analysis. *Postgrad. Med. J.* **99**(1171), 375–383. https://doi.org/10.1136/postgradmedj-2021-141135 (2023).
14. Luengo-Matos, S. et al. Efficacy and safety of robotic spine surgery: Systematic review and meta-analysis. *J. Orthop. Traumatol.* **23**(1), 49. https://doi.org/10.1186/s10195-022-00669-0 (2022).
15. Wang, H. et al. Precision insertion of percutaneous sacroiliac screws using a novel augmented reality-based navigation system: A pilot study. *Int. Orthop.* **40**(9), 1941–1947. https://doi.org/10.1007/s00264-015-3028-8 (2016).
16. Ogawa, H., Hasegawa, S., Tsukada, S. & Matsubara, M. A pilot study of augmented reality technology applied to the acetabular cup placement during total hip arthroplasty. *J. Arthroplasty* **33**(6), 1833–1837. https://doi.org/10.1016/j.arth.2018.01.067 (2018).
17. Liu, H., Auvinet, E., Giles, J. & Baena, R. Y. Augmented reality based navigation for computer assisted hip resurfacing: A proof of concept study. *Ann. Biomed. Eng.* **46**(10), 1595–1605. https://doi.org/10.1007/s10439-018-2055-1 (2018).
18. Frantz, T., Jansen, B., Duerinck, J. & Vandemeulebroucke, J. Augmenting Microsoft's HoloLens with vuforia tracking for neuronavigation. *Healthc. Technol. Lett.* **5**(5), 221–225 (2018).
19. Van Gestel, F. et al. Augmented reality-assisted neurosurgical drain placement (ARANED): Technical note. *Acta Neurochir. Suppl.* **131**, 267–273. https://doi.org/10.1007/978-3-030-59436-7_50 (2021).
20. Van Gestel, F. et al. The effect of augmented reality on the accuracy and learning curve of external ventricular drain placement. *Neurosurg. Focus* **51**(2), E8. https://doi.org/10.3171/2021.5.focus21215 (2021).
21. Frantz, T., Jansen, B., Vandemeulebroucke, J., Van Gestel, F., Duerinck, J., & Scheerlinck, T. An augmented reality system, an augmented reality HMD, an augmented reality method and a computer program. Belgium; WO2022144116A1 (2022).
22. Van Gestel, F. et al. Neuro-oncological augmented reality planning for intracranial tumor resection. *Front. Neurol.* **14**, 1104571. https://doi.org/10.3389/fneur.2023.1104571 (2023).
23. Schneider, M. et al. Augmented reality-assisted ventriculostomy. *Neurosurg. Focus* **50**(1), E16. https://doi.org/10.3171/2020.10.focus20779 (2021).
24. van Doormaal, T. P. C., van Doormaal, J. A. M. & Mensink, T. Clinical accuracy of holographic navigation using point-based registration on augmented-reality glasses. *Oper. Neurosurg. (Hagerstown)* **17**(6), 588–593. https://doi.org/10.1093/ons/opz094 (2019).
25. Fick, T., van Doormaal, J. A. M., Hoving, E. W., Regli, L. & van Doormaal, T. P. C. Holographic patient tracking after bed movement for augmented reality neuronavigation using a head-mounted display. *Acta Neurochir. (Wien)* **163**(4), 879–884. https://doi.org/10.1007/s00701-021-04707-4 (2021).
26. Felix, B. et al. Augmented reality spine surgery navigation: increasing pedicle screw insertion accuracy for both open and minimally invasive spine surgeries. *Spine* **47**(12), 865–872. https://doi.org/10.1097/BRS.0000000000004338 (2022).
27. Kriechling, P. et al. Augmented reality through head-mounted display for navigation of baseplate component placement in reverse total shoulder arthroplasty: A cadaveric study. *Arch. Orthop. Trauma Surg.* **143**(1), 169–175. https://doi.org/10.1007/s00402-021-04025-5 (2023).
28. Kurosaka, K. et al. Does augmented reality-based portable navigation improve the accuracy of cup placement in THA compared with accelerometer-based portable navigation? A randomized controlled trial. *Clin. Orthop. Relat. Res.* **481**(8), 1515–1523. https://doi.org/10.1097/CORR.0000000000002602 (2023).
29. Kunz, C. et al. Infrared marker tracking with the HoloLens for neurosurgical interventions. *Curr. Dir. Biomed. Eng.* **6**(1), 20200027. https://doi.org/10.1515/cdbme-2020-0027 (2020).
30. Gsaxner, C., Li, J., Pepe, A., Schmalstieg, D., & Egger, J. Inside-out instrument tracking for surgical navigation in augmented reality. In Proceedings of the 27th ACM Symposium on Virtual Reality Software and Technology (VRST '21). Association for Computing Machinery, New York, NY, USA, Article 4, 1–11 (2021). https://doi.org/10.1145/3489849.3489863
31. Martin-Gomez, A. et al. STTAR: Surgical tool tracking using off-the-shelf augmented reality head-mounted displays. *IEEE Trans. Vis. Comput. Graph* https://doi.org/10.1109/TVCG.2023.3238309 (2023).
32. Azimi, E., Qian, L., Navab, N., & Kazanzides, P. Alignment of the Virtual Scene to the Tracking Space of a Mixed Reality Head-Mounted Display (2019). arXiv:1703.05834https://doi.org/10.48550/arXiv.1703.05834
33. Moise, E. E. Arcs of Circles. In *Elementary Geometry from an Advanced Standpoint* 2nd edn 192–197 (Addison Wesley Publishing Company, 1974).
34. Akaike, H. A new look at the statistical model identification. *IEEE Trans. Autom. Control* **19**(6), 716–723. https://doi.org/10.1109/TAC.1974.1100705 (1974).
35. Neuville, Q., Scheerlinck, T., & Duerinck, J. Current status and future perspectives for augmented reality navigation in neurosurgery and orthopedic surgery. In P Boulanger (Ed.). Applications of Augmented Reality - Current State of the Art. United Kingdom: IntechOpen (2023). https://doi.org/10.5772/intechopen.1002344
36. Wolf, J. et al. How different augmented reality visualizations for drilling affect trajectory deviation, visual attention, and user experience. *Int. J. Comput. Assist. Radiol. Surg.* **18**(8), 1363–1371. https://doi.org/10.1007/s11548-022-02819-5 (2023).
37. Seibold, M., Spirig, J. M., Esfandiari, H., Farshad, M. & Fürnstahl, P. Translation of medical AR research into clinical practice. *J. Imaging.* **9**(2), 44. https://doi.org/10.3390/jimaging9020044 (2023).

Author contributions

All listed authors have made substantial contributions to the presented work. Research design: F.V.G., F.V.A.,

T.F., J.D., T.S.. Acquisition of data: F.V.G., F.V.A., T.F., A.V., B.J., J.V., J.D., T.S.. Analysis and interpretation of data: F.V.G., F.V.A., T.F., A.V., K.B., T.S.. Drafting the paper: F.V.G., F.V.A., T.F., A.V., T.S.. Critically revising the paper: F.V.G., K.B., B.J., J.V., J.D., T.S.. All authors have read and approved the final submitted manuscript.

Funding

The SARA research project was funded by the Flemish government through the ICON (Interdisciplinary Cooperative Research) program, provided by Flanders Innovation & Entrepreneurship and imec NPO (Interuniversity Microelectronics Centre). There was no involvement from the funders in the study design, collection, analysis and interpretation of data, the writing of this article, or the decision to submit it for publication.

Declarations

Competing interests

The authors declare no competing interests.

Additional information

Correspondence and requests for materials should be addressed to F.V.G.

Reprints and permissions information is available at www.nature.com/reprints.

Publisher's note Springer Nature remains neutral with regard to jurisdictional claims in published maps and institutional affiliations.